ARTICLE

Group 13 ion coordination to pyridyl models NAD$^+$ reduction potential

Received 00th January 20xx,
Accepted 00th January 20xx

DOI: 10.1039/x0xx00000x

Leo W. T. Parsons,[a] James C. Fettinger,[a] and Louise A. Berben*[a]

Pyridine is ubiquitous in biology as a component of the organic cofactor NAD$^+$. Herein, N-alkylation and N-metallation of pyridine are explored to understand how metal-ligand complexes can model NAD$^+$ redox chemistry. Syntheses of substituted dipyrazolylpyridine (pz_2P) compounds are reported for $(pz_2P)Me^+$ ($\mathbf{1}^+$) and $(pz_2P)GaCl_2^+$ ($\mathbf{2}^+$), and those are compared with $(pz_2P)AlCl_2(THF)^+$ and transition element pz_2P complexes from previous reports. Cyclic voltammetry measurements of $\mathbf{1}^+$ and $\mathbf{2}^+$ show irreversible reduction events that are roughly ~900 mV anodic relative to reduction of pz_2P complexes of divalent metals. We conclude that N-metallation using Group 13 ions of 3+ charge can provide an electrochemical model for N-alkylated pyridyls like NAD$^+$.

Synthetic pyridyl redox chemistry is inspired by the chemistry of nicotinamide adenine dinucleotide (NAD$^+$) and nicotinamide adenine dinucleotide phosphate (NAD(P)$^+$) that actively participate in electron transfer (ET) and proton transfer (PT) chemistry in NAD$^+$[1] and NAD(P)$^+$ dependent enzymes (Chart 1).[2] Pyridyl-based reagents now perform a wide range of redox transformations including hydride transfer,[3] and proton-coupled electron transfer (PCET)[4,5,6] as in reduction of CO_2 by pyridine derivatives with acridine (Acr) and phenanthridine (Phen) (Chart 1).[7] In these hydride transfer reactions two successive ET reactions at pyridinium followed by PT afford dihydropyridinate and large overpotentials are needed to drive ET for catalyst turnover as in CO2 reduction.[8,9,10]

This work explores the effect of various metal ions on the structure and reduction potential of pyridine.[11] Tridentate pyridine centred ligands take advantage of the chelate effect to obtain stable metal-pyridyl interactions. We chose a tridentate 2,6-dipyrazolylpyridine (pz_2P) scaffold for this work because the pyridyl central ring has flanking donor groups that are inert to both ET and PT so that chemistry can be localized on the central pyridyl (Chart 1, right).[12,13,14,15] Coordination compounds of pz_2P are reported largely with transition element ions and focus on the metal-centred reaction chemistry.[16,17,18,19] Herein, we compare the redox inert ions Al^{III}, Ga^{III} and Zn^{II} which can promote pyridyl centred redox chemistry as in NAD$^+$.[20,21] We demonstrate that these redox inert d^0 or d^{10} ions affect pyridyl electronic structure similarly to N-alkylation of pyridyl (Chart 1). Using cyclic voltammetry, we demonstrate that pz_2P complexes of Al^{III} and Ga^{III} provide the best match with the reduction potential for N-methylated pyridyl, with the reduction potential shifted anodically by ~900 mV relative to the pz_2P complexes of Zn^{II},[22] and other divalent ions.[23] This contribution sets the stage for future detailed mechanistic work on the PCET chemistry of NAD$^+$ models using electrochemical techniques. Prior work has used chemical reagents as redox mediators, which are known to be chemically non-innocent.[24]

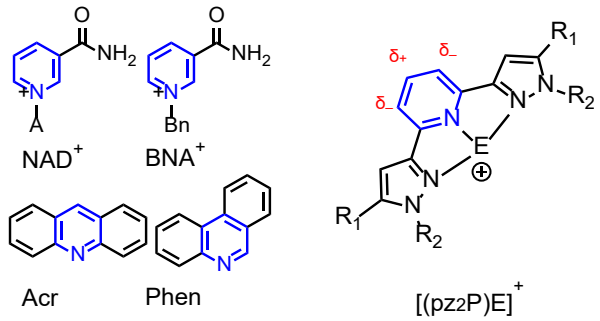

Chart 1. Line drawings: (left) representative pyridyl-based redox mediators. A = Adenine Dinucleotide. (right) of $[(pz_2P)E]^+$. E is a d^0 or d^{10} metal ion (Al^{III}, Ga^{III}) or alkyl.

Synthesis of $\mathbf{1}^+$ and $\mathbf{2}^+$ were achieved starting from isolated pz_2P. *N*-Methylation to form pyridinium or imidazolium salts is often achieved by reaction of pyridine or imidazole with excess methyl iodide (MeI).[25,26] However, reaction of pz_2P with one equivalent methyl iodide in THF yielded no methylated product at room temperature or upon heating to 50 °C over 24 hours. Addition of one equivalent of methyl triflate (MeOTf) to pz_2P in toluene led to precipitation of a white powder identified as [pz_2(*N*-MeP)]OTf (**1**-OTf) in 83 % yield based on ^{1}H and ^{13}C NMR spectra (Scheme 1). *N*-Methylation was evident by observation of a new ^{1}H resonance at 4.50 ppm which integrated to 3H against the individual pyridyl and pyrazine protons. A single

[a] *Department of Chemistry, University of California, Davis CA 95616, USA*
Electronic Supplementary Information (ESI) available: Synthesis and characterization of compounds, ^{1}H and ^{13}C NMR, electrochemical data, tables of crystallographic data, crystallographic data (CIF). CCDC 2264174 and 2264175 contains the supplementary crystallographic data for this paper. These data can be obtained free of charge from the Cambridge Crystallographic Data Centre via www.ccdc.cam.ac.uk/data_request/cif. See DOI: 10.1039/x0xx00000x

pyrazole proton signal is observed at 6.68 ppm in C_6D_6, indicating a mirror plane of symmetry in the molecule which is consistent with selective *N*-methylation of the central pyridine and no methylation of the pyrazole *N*-atoms (Figure S1).

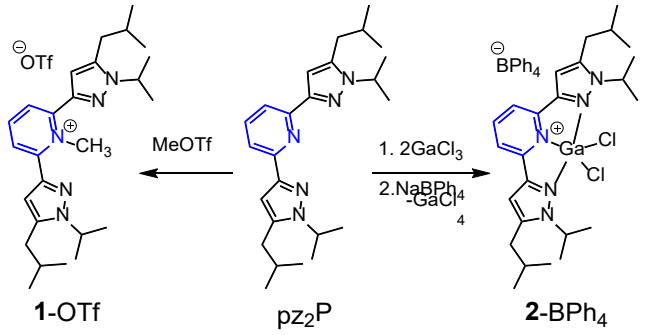

Scheme 1: Synthesis of neutral pz_2P complexes **1**-OTf~~, **2**-$GaCl_4$~~ and **2**-BPh_4.

Synthesis of $[(pz_2P)GaCl_2]GaCl_4$ (**2**-$GaCl_4$) was achieved by addition of two equivalents of $GaCl_3$ dissolved in THF to a solution of pz_2P in THF (Scheme 1). After 1 h, the THF was evaporated and the residue was triturated in Et_2O, and **2**-$GaCl_4$ was collected as a white powder in 80% yield (see SI for full synthetic details). The ^{1}H NMR spectra of **2**-$GaCl_4$ indicates there is no coordinated THF solvate which is different to the prior report of $[(pz_2P)AlCl_2(THF)]AlCl_4$ (**A**-$AlCl_4$) (Figure S2).[27] Single crystals obtained from saturated solutions of **2**-$GaCl_4$ were consistently of poor quality so a metathesis reaction of **2**-$GaCl_4$ with sodium tetraphenylborate ($NaBPh_4$) was performed to isolate $[(pz_2P)GaCl_2]BPh_4$ (**2**-BPh_4) in 69% yield. The proton NMR spectrum of **2**-BPh_4 showed at 7.40, 6.88 and 6.71 ppm for 8H, 8H and 4H aryl protons, respectively, corresponding to the aryl protons of BPh_4^-. A quartet at 164.55 ppm was also in the ^{13}C NMR spectra in $CDCl_3$ arising from ^{11}B – ^{13}C coupling (Figure S3).

An effect of the N heteroatom in pyridine is a withdrawal of electron density so that pyridyl ^{1}H NMR resonances are inequivalent and appear over a wide range, relative to aromatic hydrocarbons such as toluene. The C_o-H, C_m-H, and C_p-H signals appear at 8.53, 6.66, and 6.98 ppm, respectively, for pyridine and the C_o-H/C_p-H and C_m-H signals appear at and 7.02 and 7.13 for toluene in C_6D_6 (atom labelling scheme is shown in Chart 2).[28] As a metric for the polarization of the pyridyl ring by the N heteroatom we focus on the difference in the C_m-H and C_p-H ^{1}H NMR signals in C_6D_6, denoted as $\Delta\delta(C_m\text{-}C_p)$; smaller differences indicate more even electron shielding as a result of more equal distribution of electron density in the aromatic ring. For pyridine and toluene $\Delta\delta(C_m\text{-}C_p)$ are 0.32 and 0.11, respectively.

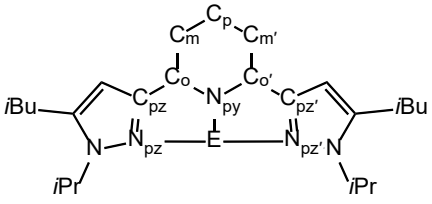

Chart 2. Atom labelling scheme in pz_2P and derivatives that are discussed throughout this work.

For $\mathbf{1}^+$, $\mathbf{2}^+$, or $\mathbf{A}^+$, the C_p-H resonance is observed at 7.61, 8.03, and 7.97 ppm, respectively, which is upfield from 8.27 ppm in pz_2P and is consistent with greater electron density at the C_p atom upon *N*-alkylation or *N*-metallation. The C_m-H resonances in $\mathbf{1}^+$, $\mathbf{2}^+$, or $\mathbf{A}^+$ are at 7.77, 7.84 and 7.52 ppm, respectively, which is a downfield shift from 7.34 ppm in pz_2P. The $\Delta\delta(C_m\text{-}C_p)$ are 0.93, 0.09, 0.20, and 0.19 ppm for pz_2P, $\mathbf{1}^+$, $\mathbf{2}^+$, and $\mathbf{A}^+$, respectively, where generally more uniform electron density across the pyridine ring arises from coordination to E. Moreover, the effect of *N*-alkylation or $AlCl_2^+$ or $GaCl_2^+$ coordination on pz_2P are similar. Data reported in C_6D_6 for $(pz_2P)ZnCl_2$ shows that $\Delta\delta(C_m\text{-}C_p)$ = 0.27 ppm (where R_1 = *t*Bu and R_2 = 9-propyl-9-borobicyclo[3.3.1]nonyl, Chart 1), indicating a similar electronic effect of pz_2P coordination to $ZnCl_2$.[22]

Solid-state structures. Crystals of **1**-OTf and **2**-BPh_4 suitable for single crystal X-ray diffraction were obtained from saturated solutions of THF layered with hexanes as colourless blocks and as yellow blocks, respectively (Tables S1, S2 and Figure 1). The structure of **1**-OTf shows that the N-pyrazolyl donor atoms are facing in toward the *N*-methyl group and that the methyl group lies out of the plane of the pyridine ring by 9.2°. The structure of **2**-BPh_4 confirms its formulation as a five-coordinate Ga centre comprised of the 3 N-donors of the pz_2P ligands and two chloride ligands. The absence of a THF solvate on the Ga centre in **2**-BPh_4 is in contrast to the structure of **A**-$AlCl_4$ and suggests that the Ga centre is less Lewis acidic than the Al centre in **A**-$AlCl_4$.[27] The coordination geometry about Ga is in between square pyramidal and trigonal bipyramidal, where τ_5 is 0.586.[29] The N_{pz}-C_{pz}-$C_{pz'}$-$N_{pz'}$ torsion angle is 167.32° for **2**-BPh_4 and is slightly larger than that observed for 6-coordinate **A**-$AlCl_4$ (171.18°). A comparison of the pyridyl bond lengths in $\mathbf{1}^+$, $\mathbf{2}^+$, and **A**-$AlCl_4$ with those in NAD^+ was not insightful due to the large errors and variability of the bond length metrics in the structures of published NAD^+ structures (Calculation S2 and Figure S4).

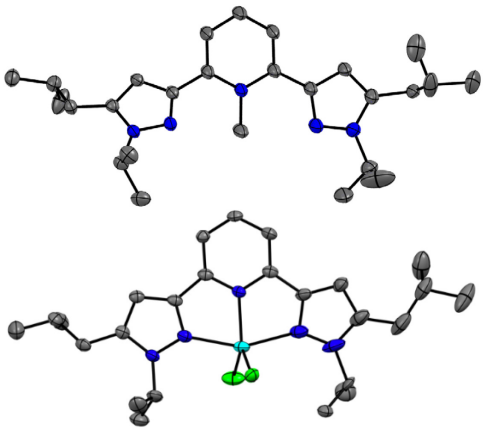

Figure 1: Solid state structures of **1**-OTf (top) and **2**-BPh_4 (bottom). Blue, gray, teal and green ellipsoids represent N, C, Ga, and Cl atoms, respectively. The thermal ellipsoids are shown at 30% probability. Hydrogen atoms and counter ions excluded for clarity.

Electrochemistry Measurements. Cyclic voltammetry (CV) was used to characterize the behaviour of **1**-OTf, **2**-$GaCl_4$, **A**-$AlCl_4$, and pz_2P in 0.3 M Bu_4NBF_4 THF solution, and of **1**-OTf**, 2**-$GaCl_4$, and pz_2P in 0.1 M Bu_4NBF_4 MeCN solution (Figure 2). **A**-

$AlCl_4$ is not stable in MeCN solution.[27] All of the redox features were irreversible. In THF the reduction peak potentials (E_{pc}) for **1**-OTf, **2**-$GaCl_4$, and **A**-$AlCl_4$, are -1.11, -0.98, -1.13 V vs. SCE respectively, and no reduction event was observed within the solvent window for pz_2P in THF. For **A**-$AlCl_4$ the E_{pc} is 150 mV more cathodic than for $\mathbf{2}^+$ and we attribute this difference to the increased affinity of **A**-$AlCl_4$ for THF as evidenced by the THF solvate in the solid-state structure of **A**-$AlCl_4$. Similarly, the instability of **A**-$AlCl_4$ in MeCN may arise from the greater Lewis acidity of **A**-$AlCl_4$ relative to $\mathbf{2}^+$ which is surprisingly stable in MeCN. In MeCN solution **1**-OTf and **2**-$GaCl_4$, have E_{pc} at -1.20 and -1.03 V vs SCE respectively, and no reduction event was observed within the solvent window for pz_2P.

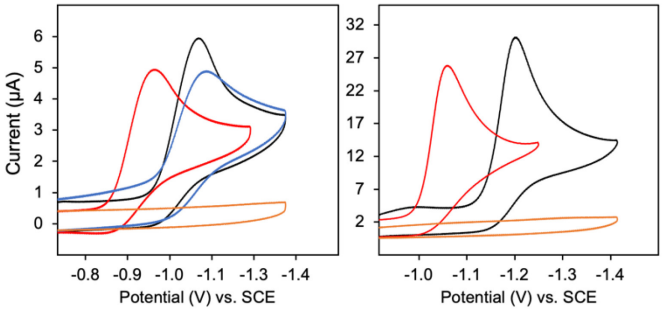

Figure 2. (left) CV's of 0.5 mM **1**-OTf (black), **2**-$GaCl_4$ (red), **A**-$AlCl_4$ (blue), and pz_2P (gold) recorded at 0.1 Vs^{-1} in 0.3 M Bu_4NBF_4 THF. (right) CV's of 0.5 mM **1**-OTf (black) **2**-$GaCl_4$ (red), and pz_2P (gold) recorded at 0.1 Vs^{-1} in 0.1 M Bu_4NBF_4 MeCN

The E_{pc} values observed here are consistent with reported values for reduction of other *N*-alkylated pyridinium cations,[30,31] and with potentials we reported previously where ET is ligand based in bis(imino)pyridine Al(III) and Ga(III) complexes.[32,33] Taken together, this context supports assignment of the irreversible reduction events of **1**-OTf, **2**-$GaCl_4$, and **A**-$AlCl_4$ as pyridine-based. Further, the E_{pc} values in the trivalent Al and Ga ion complexes of pz_2P closely match that for *N*-alkylated **1**-OTf. According to prior reports, ligand based reductive peak potentials are much more negative when pz_2P ligands are coordinated to divalent metals. As examples, Caulton and coworkers reported E_{pc} = -2.08 V vs SCE in THF, and Szymczak and coworkers reported E_{pc} = -1.84 V vs SCE in 0.2 M Bu_4NPF_6 THF, for Fe^{II},[23] and Zn^{II},[22] complexes of pz_2P, respectively. Those E_{pc} values are 700 - 1000 mV more negative than those for **1**-OTf. Complexes of pz2P with the transition metals display metal-based reductions.[34,35,36]

It is common for synthetic model compounds of NAD^+ to display irreversible CV traces.[37,38,39] This can lead to challenges in determining $E_{1/2}$, although in some cases, at high scan rates (>10,000 Vs^{-1}) and high concentrations (> 1 mM) partial reversibility of the reduction wave for nicotinamide, acridine and quinone organic NAD^+ models can be achieved.[40] We were unable to achieve reversibility in the current work with concentrations up to 1 mM and scan rates up to 20 Vs^{-1} using a standard glassy carbon button electrode in MeCN solution (Figure S5). The irreversibility of the CV traces potentially stems from a couple different origins, and these include slow ET kinetics, or a chemical reaction which immediately proceeds the ET event to consume **1**, **2** and **A** which were generated by electrochemical reduction from **1**-OTf, **2**-$GaCl_4$ and **A**-$AlCl_4$, respectively. In experiments designed to probe the irreversibility, changes in E_{pc} with increasing scan rate were recorded (Figure 3). Plots of current density (j_{pc}) vs. $\upsilon^{0.5}$, for **1**-OTf, **2**-$GaCl_4$ and **A**-$AlCl_4$ in THF, are linear and this indicates a diffusion-controlled process (Figure S6, Calculation S1). We further observed that E_{pc} shifts anodically with increasing υ, and this suggests that an irreversible chemical step likely follows ET on the CV timescale (equations 1 – 3). There are two likely chemical reactions that could follow ET and those are protonation (by trace water) or dimerization:

$$[(pz_2P)E]^+ + e^- \rightarrow (pz_2P)E \qquad \text{eqn 1}$$

$$(pz_2P)E + H^+ \rightarrow (pz_2HP)E \qquad \text{eqn 2}$$

$$(pz_2P)E \rightarrow \tfrac{1}{2}\,[(pz_2P)E]_2 \qquad \text{eqn 3}$$

To determine which of these chemical reactions is occurring after ET we investigated the order of the reaction with respect to **1**-OTf, **2**-$GaCl_4$ and **A**-$AlCl_4$. Since ET is fast, an order dependence of 1 with respect to the analyte will be seen if PT is operative (equation 2), and an order of 2 with respect to the analyte will be observed in the case of dimerization (equation 3). Plots of j_{pc} vs concentration of **1**-OTf and **2**-$GaCl_4$ in the presence of protons show a linear relationship, and support assignment of PT (equation 2) as a possible chemical step following ET as the cause of irreversibility in the CV (Figure S7).

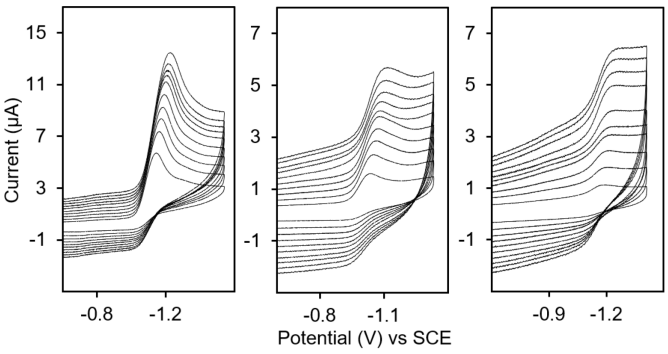

Figure 3. CV traces of **1**-OTf (left), **2**-$GaCl_4$ (middle), **A**-$AlCl_4$ (right) in 0.3 M Bu_4NBF_4 THF solution with scan rates 0.1 to 1.0 Vs^{-1}. This data was used to determine a diffusion-controlled process (Figure S5 and equation S1) with an irreversible chemical step following ET.

N-methylated and *N*-metalated pyridyl-ligand compounds have been isolated. In each structure the central *N*-functionalized pyridine ring is supported by two flanking pyrazolyl ligands that enhance stability of the compounds. The cationic compounds, **1**-OTf, **2**-$GaCl_4$ and **A**-$AlCl_4$, have the form $[(pz_2P)E]^+$ where E = $AlCl_2^+$, $GaCl_2^+$, and CH_3^+, respectively. All three compounds have similar proton NMR resonances and structural features and differ from known transition element pz_2P complexes. Irreversible reduction events with E_p between -0.98 and -1.13 V were observed for each of **1**-OTf, **2**-$GaCl_4$ and **A**-$AlCl_4$ in THF solution and demonstrate that trivalent Group 13

cations are good models for the reduction chemistry of *N*-alkylated pyridine. Our future work will harness these model compounds in understanding PCET mechanisms of NAD^+-inspired dihydropyridinate chemistry.

Conflicts of interest

No conflicts to declare.

Acknowledgements

This manuscript is based on work supported by the National Science Foundation with award CHE-2054529

Notes and references

1 [1] A. Dolega, *Coord. Chem. Rev*., 2010, **254**, 916–937.
2 [2] L. S. Vidal, C. L. Kelly, P. M. Mordaka and J. T. Heap, *Biochim. Biophys. Acta, Proteins Proteomics,* 2018, **1866**, 327−347.
3 [3] E. J. Lawrence, E. R. Clark, L. D. Curless J. M. Courtney, R. J. Blagg, M. J. Ingleson and G. G. Wildgoose, *Chem. Sci.*, 2016, **7**, 2537–2543.
4 [4] P. T. Smith, S. Weng and C. J. Chang, *Inorg. Chem*., 2020, **59**, 9270-9278.
5 [5] C-H. Lim, A. M. Holder, J. T. Hynes and C. B. Musgrave, *J. Am. Chem. Soc.,* 2014, **136**, 16081-16095.
6 [6] A. Marjolin, and J. A. Keith, *ACS Catal*., 2015, **5**, 1123-1130.
7 [7] P. K. Giesbrecht and D. E. Herbert, *ACS Energy Lett*., 2017, **2**, 549-555.
8 [8] S. Ilic, U. P. Kadel, Y. Basdogan, J. A. Keith and K. D. Glusac, *J. Am. Chem. Soc*., 2018, **140**, 4569-4579.
9 [9] S. Ilic, A. Alherz, C. B. Musgrave and K. D. Glusac, *Chem. Soc. Rev.,* 2018, **47**, 2809-2836.
10 [10] S. Ilic, A. Alherz, C. B. Musgrave and K. D. Glusac*, Chem. Commun.,* 2019, **55**, 5583-5586.
11 [11] B. L. Thompson and Z. M. Heiden, *Phys. Chem. Chem. Phys.*, 2021, **23**, 9822-9831.
12 [12] M. A. Halcrow, *Coord. Chem. Rev*., 2005, **249**, 2880-2908.
13 [13] A. V. Polezhaev, C-H. Chen, A. S. Kinne, A. C. Cabelof, R. L. Lord and K. G. Caulton, *Inorg. Chem*., 2017, **56**, 9505-9514.
14 [14] C. Groß, Y. Sun, T. Jost, T. Grimm, M. P. Klein, G. Niedner-Schatteburg, S. Becker and W. R. Thiel, *Chem. Commun.,* 2020, **56**, 368-371.
15 [15] S. Radisavljevic, L. Bratsos, A. Scheurer, J. Korzekwa, R. Masnikosa, A. Tot, N.Gligorijeciv, S. Radulovic and A. R. Simovic, *Dalton Trans.,* 2018, **47**, 13696-13712.
16 [16] P. Weingart, P. Hutchen, A. Damone, M. Kohns, H. Hasse and W. R. Thiel, *ChemCatChem,* 2020, **12**, 3913-3928.
17 [17] Y. Pankratova, D. Aleshin, I. Nikovskiy and Y. Nelyubina, *Inorg. Chem*., 2020, **59**, 7700-7709.
18 [18] N. Suryadevara, A. Mizuno, L. Spieker, S. Salamon, S. Sleziona, A. Maas, E. Pollmann, B. Heinrich, M. Schleberger, H. Wende, A. K. Kuppusamy and M. Ruben, *Chem. Eur. J*., 2022, **28**, e2021035835.
19 [19] J. J. Kiernicki, M. Zeller, and N. K. Szymczak, *Inorg. Chem*., 2020, **59**, 9279-9286.
[20] C. D. Cates, T. W. Myers, L. A. Berben, *Inorg. Chem*. 2012, **51**, 11891-11897.
20 [21] T. W. Myers, L. A. Berben, *Chem. Commun*. 2013, **49**, 4175-4177.
21 [22] J. J. Kiernicki, M. Zeller and N. Szymczak, *J. Am. Chem. Soc.,* 2017, **139**, 18194-18197.
22 [23] B. J. Cook, C-H. Chen, M. Pink, R. L. Lord and K. G. Caulton, *Inorg. Chim. Acta*, 2016, **451**, 82-91.
23 [24]M. A. Martini, O. Rudiger, N. Breuer, B. Nöring, S. DeBeer, P. Rodríguez-Maciá and J. A. Birrell, *J. Am. Chem. Soc*., 2021, **143**, 18159–18171.
24 [25] H. Peng, T. Li, D. Tian, H. Yang, G. Xu and W. Tang, *Org. Biomol. Chem*., 2021, **19**, 4237-4337.
25 [26] D. Jo, and S. H. Hong, *Chem. Commun*., 2018, **45**, 487-490.
[27] T. J. Sherbow, J. C. Fettinger and L. A. Berben, Inorg. Chem., 2019, 56, 8651-8660.
26 [28] G. R. Fulmer, A. J. M. Miller, N. H. Sherden, H. E. Gottlieb, N. Nudelman, B. M. Stoltz, J. E. Bercaw and K. I. Goldberg, *Organometallics,* 2010, **29**, 2176-2179.
27 [29] A. W. Addison, T. N. Rao, J. Reedijk, J. van Rijin and G. C. Verschoor, *J. Chem Soc Dalton Trans*., 1984, **7**, 1349-1356.
28 [30] X-Q. Zhu, Y. Tan and C-T. Cao, *J. Phys Chem. B*, 2010, **114**, 2058-2075.
29 [31] H. Zhao, Y. Li and X-Q. Zhu, *ACS Omega*, 2018, **3**, 13598-13608.
30 [32] T. W. Meyers and L. A. Berben, *Inorg. Chem*., 2012, **51**, 1480-1488.
31 [33] A. Arnold, T. J. Sherbow, R. I. Sayler, R. D. Britt, E. J. Thompson, M. T. Munoz, J. C. Fettinger and L. A. Berben, *J. Am. Chem. Soc*., 2019, **141**, 15792-15803.
32 [34] N. S. Labrum, J. Seo, C-H. Chen, M. Pink, D. M. Began and K. G. Caulton, *Inorg*. *Chem*. *Acta*, 2019, **486**, 483-491.
33 [35] J. Korzekwa, A. Scheurer, F. W. Heinemann and K. Meyer, *Dalton Trans*., 2017, **46**, 13811-13823.
34 [36] B. J. Cook, M. Pink, K. Pal, and K. G. Caulton, *Inorg. Chem*., 2018, **57**, 6176-6185.
35 [37] J-D. Yang, B-L. Chen and X-Q. Zhu, *J. Phys. Chem. B,* 2018, **122**, 6888-6898.
36 [38] X-Q. Zhu, M-T. Zhang, A. Yu, C-H. Wang and J-P. Cheng, *J. Am. Chem. Soc*., 2008, **130**, 2501-2516.
37 [39] X-Q . Zhu, Y. Tan and C-T. Cao, *J. Phys Chem. B*, 2010, **114**, 2058-2075.
38 [40] A. Anne, P. Hapiot and J.-M. Saveant, *J. Electroanal. Chem.* 1991, **221**, 959-970.

